

Dehydrocoupling of Dimethylamine-Borane Promoted by Manganese(II) *m*-Terphenyl Complexes

Helen R. Sharpe,^a Ana M. Geer,^a Toby J. Blundell,^a Fiona R. Hastings,^a Michael W. Fay,^b Graham A. Rance,^b William Lewis,^a Alexander J. Blake^a and Deborah L. Kays,^{a*}

^a School of Chemistry, University of Nottingham, University Park, Nottingham, NG7 2RD, UK.

^b Nanoscale and Microscale Research Centre, University of Nottingham, University Park, Nottingham, NG7 2RD, UK

Email: Deborah.Kays@nottingham.ac.uk

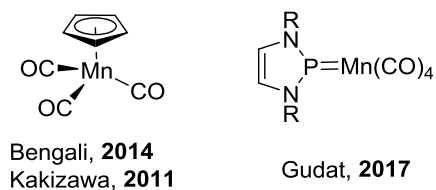
Electronic Supplementary Information (ESI) available: selected spectra, %V_{Bur} calculations, NMR reaction monitoring, crystallographic data and CIF files. CCDC-1548834. See DOI: 10.1039/C7CY02086D.

Abstract

Two- and three-coordinate manganese *m*-terphenyl complexes are precatalysts for the dehydrogenation of dimethylamine-borane (Me₂NH·BH₃) affording one equivalent of molecular hydrogen and half an equivalent of [Me₂N–BH₂]₂. Experimental studies into the nature of the catalyst indicate that small changes in the coordination environment give rise to significant differences in the reaction mechanism, occurring through a homogeneous mechanism for two-coordinate precatalysts, whilst for the three-coordinate species a heterogeneous mechanism takes place where nanoparticles are responsible for the catalysis.

Introduction

The catalytic dehydrocoupling of amine-boranes has gained considerable significance in the last decade because of their potential application as hydrogen storage materials.¹ These molecules contain a high weight percentage of hydrogen, which, in conjunction with the electronegativity difference between nitrogen and boron (inducing protic N–H and hydridic B–H bonds), permits the release of hydrogen at high temperatures or mediated by a catalyst. Furthermore, amine-boranes have applications as hydrogen transfer reagents² and precursors to BN-based ceramics and polymeric materials.³ Most of the catalysts for this transformation contain precious metals, which are expensive, scarce and toxic.⁴ Recently, abundant first row transition elements have been used as catalysts for dehydrogenation reactions, although many of these require photoirradiation in order to initiate the reaction. There has been a special interest in iron precatalysts;⁵ in particular the use of carbonyl species, [CpFe(CO)₂]₂ and CpFe(CO)₂I (Cp = η⁵-C₅H₅), where structural variations in the precatalysts result in a homogeneous or heterogeneous reaction mechanism.^{5b} A limited number of cobalt precatalysts have also been reported to dehydrocouple amine-boranes; these include Cp*Co(CO)I₂ (Cp* = η⁵-C₅Me₅), which is active under aerobic conditions.⁶ Manganese catalysts are significantly underutilised for dehydrogenation reactions. CpMn(CO)₃ catalyses amine-borane dehydrocoupling (Figure 1),⁷ although the reaction requires photoactivation and long reaction times.



Catalysts used in this work:

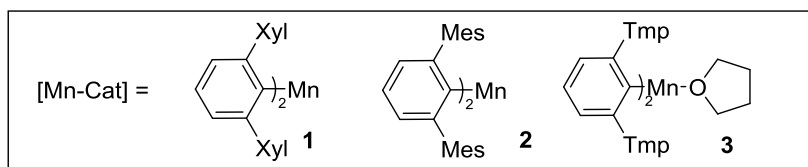


Figure 1. Previous examples of manganese complexes used for amine-borane dehydrogenation and *m*-terphenyl manganese complexes **1-3** (Xyl = 2,6-Me₂C₆H₃, Mes = 2,4,6-Me₃C₆H₂, Tmp = 2,4,5-Me₃C₆H₂) used in this work.

More recently, an N-heterocyclic phosphonium manganese catalyst (Figure 1) has been shown to be active for ammonia borane dehydrogenation, with substrate activation through an unusual ligand-centred pathway, where the substrate transfers hydrogen to the phosphorus atom and one nitrogen atom of the phosphonium ligand.⁸ There is an increasing interest in catalysts based on manganese due to its high natural abundance and biocompatibility.⁹ In this context, we have recently disclosed manganese(II) *m*-terphenyl complexes as effective catalysts for the cyclotrimerisation of aliphatic isocyanates under mild conditions, operating through a Lewis acid mechanism.¹⁰ Herein, we report the dehydrogenation/dehydrocoupling of dimethylamine-borane (Me₂NH·BH₃) catalysed by two- and three-coordinate manganese(II) *m*-terphenyl complexes (**1-3**) under mild conditions (Scheme 1). Small changes in the metal coordination sphere have considerable impact on the reaction, which can operate either through a homogeneous or heterogeneous mechanism.

Results and discussion

The two-coordinate complex (2,6-Xyl₂C₆H₃)₂Mn (**1**) was synthesised *via* the reaction of MnBr₂ with one equivalent of [2,6-Xyl₂C₆H₃Li]₂ (Xyl = 2,6-Me₂C₆H₃) in a mixture of toluene and THF with concomitant formation of the lithium halide. Crystallisation was achieved by slow cooling of saturated hexane (Figure 2) obtaining single crystals adequate for X-ray diffraction; the Mn–C bond lengths and C–Mn–C angle for **1** [Mn(1)–C(1) = 2.089(3) Å, Mn(1)–C(23) = 2.087(3) Å and C(1)–Mn(1)–C(23) 169.57(15)°] are within the range of other two-coordinate diaryl manganese complexes in literature.¹¹ The synthesis of (2,6-Mes₂C₆H₃)₂Mn (**2**; Mes = 2,4,6-Me₃C₆H₂) and (2,6-Tmp₂C₆H₃)₂Mn(THF) (**3**; Tmp = 2,4,5-Me₃C₆H₂) were achieved by literature procedures.^{10, 11b} In order to compare the steric impact of the *m*-terphenyl ligands in these complexes, the percent buried volume (%V_{Bur}) and steric maps were calculated from the solid state structure (Figure S1, Supporting information).¹² Varying the flanking group from 2,6-Xyl to 2,6-Mes has negligible impact on the %V_{Bur} of the ligands on **1** and **2** (42.0 and 42.7, respectively). However, for complex **3**, the %V_{Bur} of the *m*-terphenyl ligand dramatically decreases to 37.5, indicating a significant reduction in the steric shielding around the metal centre. In particular, the *ortho* substituents on the outer aromatic ring provide greater steric coverage to the metal centre in **1** and **2**.

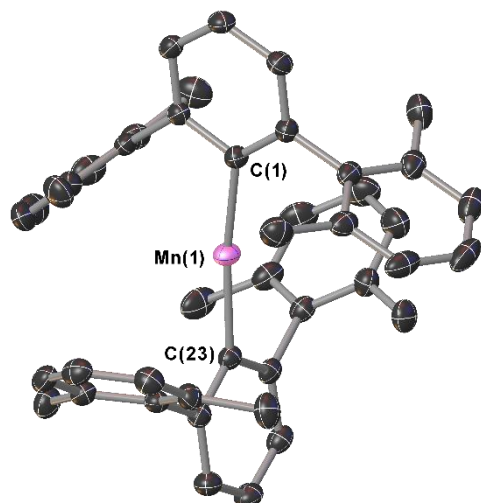
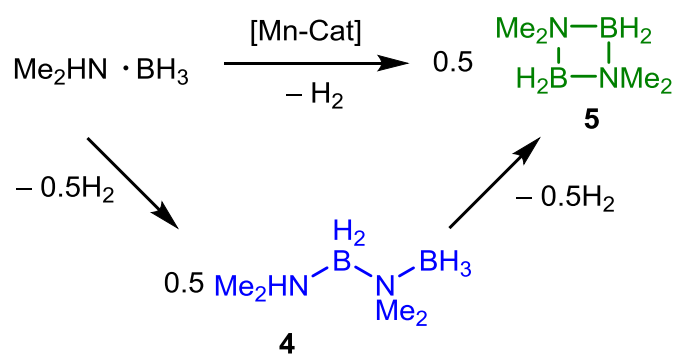


Figure 2. Molecular structure of (2,6-Xyl)₂C₆H₃)₂Mn (**1**) with anisotropic displacement parameters set at 50% probability. Hydrogen atoms have been omitted for clarity. Selected bond lengths (Å) and angles (°) for **1**: Mn(1)-C(1) 2.089(3), Mn(1)-C(23) 2.087(3), C(1)-Mn(1)-C(23) 169.57(15), Ar-Ar dihedral angle 93.91(8).

Initial dehydrocoupling experiments between **1-3** (5 mol%) and Me₂NH·BH₃ were performed in C₆D₆ at room temperature (rt); the appearance of dihydrogen bubbles in the NMR tube suggesting an immediate reaction. However, under these reaction conditions all three precatalysts gave poor conversion to products (entries 1-3, Table 1). Analysis of these reactions by ¹H and ¹¹B NMR spectroscopy after 16 h revealed conversions of 15-38%, where the major product Me₂NH-BH₂-NMe₂-BH₃ (**4**) was assigned by ¹H and ¹¹B NMR spectroscopy [δ_B 2.3 (t, J_{BH} = 109 Hz, BH₂), -13.1, (q, J_{BH} = 97 Hz, BH₃)]. In the ¹¹B NMR spectrum, the BH₃ moiety was concealed by the precursor Me₂NH·BH₃ (Figure S10, Supporting Information).¹³ This linear diborazane (**4**) is a key intermediate in the formation of the cyclic dimer [Me₂N-BH₂]₂ (**5**) for catalytic systems including Ti,¹³ Fe,^{5g} Sc,¹⁴ Ir¹⁵ and Rh.¹⁶ Increasing the temperature to 60 °C improved activity and selectivity for all three precatalysts (entries 4-6, Table 1). Precatalysts **1**, **2** and **3** completely converted Me₂NH·BH₃ into **5** in *ca.* 2 h, 4 h and 12 h, respectively. The higher proportion of **5** to the linear species **4** in the reactions performed at 60 °C compared with those at room temperature is in agreement with the latter being an intermediate to the cyclic dimer, as previously described by Manners et al.^{5g} Precatalysts **1** and **3** display high conversions when lowering the catalyst loading to 2 mol%, whilst for **2** the conversion drops to 75% and is accompanied by a larger amount of **4** (entries 7-9, Table 1).



Scheme 1 Dehydrocoupling of $\text{Me}_2\text{NH} \cdot \text{BH}_3$ using manganese(II) *m*-terphenyl precatalysts **1-3**.

Table 1. Dehydrocoupling of $\text{Me}_2\text{NH} \cdot \text{BH}_3$ with **1-3**.^{a)}

Entry	Catalyst (mol%)	T (°C)	t (h)	Conversion (%) ^{b)}	Product Ratio ^{c), d)} 4/5/6^{e)}
1	1 (5)	rt	16 ^{f)}	15	75/24/0
2	2 (5)	rt	16 ^{f)}	33	84/10/3
3	3 (5)	rt	16 ^{f)}	38	69/28/1
4	1 (5)	60	1.7	94	0/97/2
5	2 (5)	60	3.8	96	1/95/1
6	3 (5)	60	12	96	2/94/2
7	1 (2)	60	16 ^{f)}	94	1/98/1
8	2 (2)	60	16 ^{f)}	75	4/95/1
9	3 (2)	60	16 ^{f)}	99	0/99/0

^{a)} Reaction conditions: 10 mg of catalyst, 0.6 mL of C_6D_6 . ^{b)} Determined by ^1H NMR and ^{11}B NMR spectroscopy. ^{c)} Ratio by ^1H NMR and ^{11}B NMR. ^{d)} Small amounts of $\text{HB}(\text{NMe}_2)_2$ (<3%) were also detected by ^{11}B NMR. ^{e)} $\text{Me}_2\text{N}=\text{BH}_2$ (**6**). ^{f)} Samples were heated at 60 °C in an oil bath, after 16 h the progress was monitored by NMR.

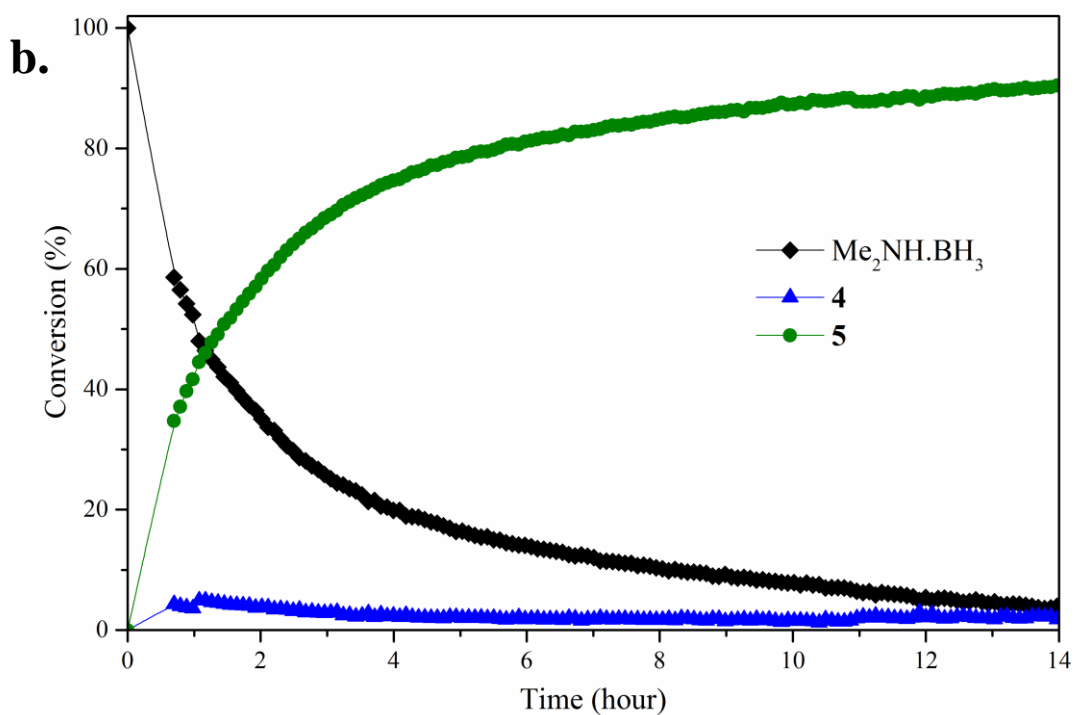
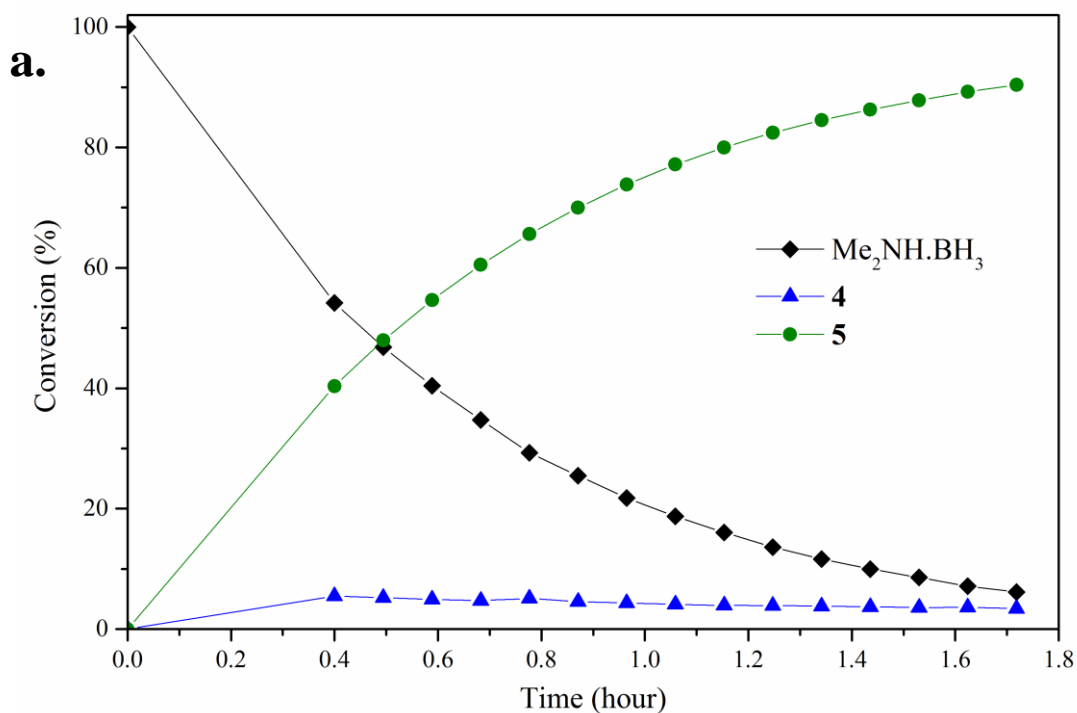


Figure 3. (a) Conversion (%) vs. time (h) for the dehydrogenation of Me₂NH·BH₃ using **1** (5 mol%) at 60 °C. (b) Conversion (%) vs. time (h) for the dehydrogenation of Me₂NH·BH₃ using **3** (5 mol%) at 60 °C. In both cases **6** and HB(NMe₂)₂ were observed in the ¹¹B NMR spectra in small quantities (<2%).

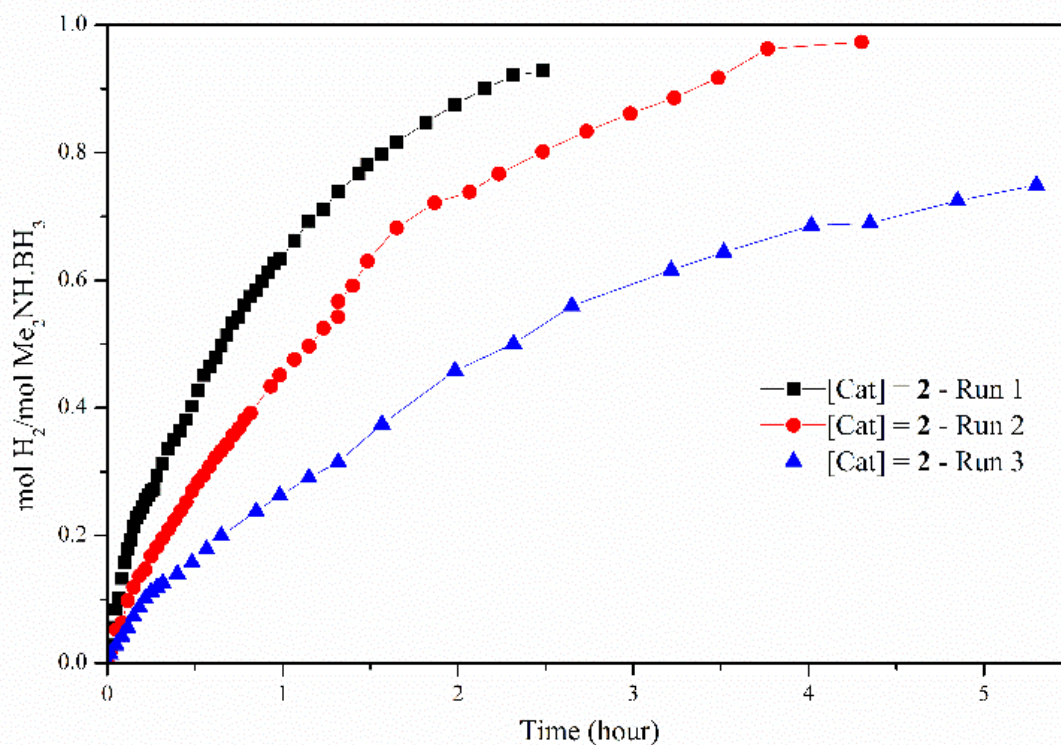


Figure 4. H₂ equivalents (molH₂/molMe₂NH·BH₃) vs. time (h) for the dehydrogenation of Me₂NH·BH₃ using **2** (7 mol%) in toluene at 60 °C.

To gain further insight into the dehydrocoupling of Me₂NH·BH₃ using precatalysts **1-3** the progress of the reactions was monitored by ¹H NMR and ¹¹B NMR spectroscopy in C₆D₆ at 60 °C (Figure 3 and Supporting Information) and by measuring the amount of H₂ formed with a gas burette (Figure 4); no induction period was observed when undertaking these experiments. Small quantities (*ca.* 2%) of the diaminoborane HB(NMe₂)₂ and the monomeric aminoborane Me₂N=BH₂ (**6**) were observed in these reactions. Significantly, monitoring the reaction of Me₂NH·BH₃ with precatalyst **3** (5 mol%, C₆D₆, 60 °C) by NMR provided mechanistic insight. Free THF is observed by ¹H NMR upon addition of Me₂NH·BH₃, indicating that the first step of the reaction is likely amine-borane coordination to the metal centre displacing labile THF. Therefore, differences in the reaction mechanisms are likely due to the changes in the *m*-terphenyl ligands. Although ammonia has been shown to cleave a M–C bond in (2,6-*i*Pr₂C₆H₃)₂Mn,¹⁷ protolytic cleavage of a metal-bound *m*-terphenyl ligand as part of the catalytic cycle has been discounted due to the lack of evidence of the formation of protonated ligand during the catalysis *via* ¹H NMR. It is conceivable that the Mn(II) centre will behave as a Lewis acid in the homogeneous reaction, similar to that seen for other low-coordinate transition metal aryl precatalysts,^{18, 10} with initial coordination of Me₂NH·BH₃ to the metal centre though interaction of BH₃ unit, similar to that for the manganese half-sandwich complexes investigated by Shimoi,^{7b} *via* a mechanism reminiscent of that for Manners' Fe(II)-catalysed system.^{5g}

Table 2. Dehydrocoupling of Me₂NH·BH₃ with **1-3** in the presence of mercury. ^{a)}

Entry	Cat. (mol%)	Time	Conversion (%) ^[b]	Product Ratio ^{[c], [d]} 4/5/6
1	1 (5%)	2 h	92	0/98/2
2	2 (5%)	4 h	90	40/60/1
3	3 (5%)	16 h	29	14/83/1

^{a)} Reaction conditions: 10 mg cat., 60 °C, 16 h, 0.6 mL of C₆D₆. ^{b)} Determined by ¹H NMR and ¹¹B NMR spectroscopy. ^{c)} Ratio by ¹H NMR and ¹¹B NMR. ^{d)} Small amounts of HB(NMe₂)₂ (<3%) were also detected by ¹¹B NMR.

Recycling studies were carried out with catalyst **2** (7 mol%, toluene, 60 °C), by addition of three consecutive loadings of Me₂NH·BH₃ after the catalysis (Figure 4). Comparable conversions are obtained on the second run, but the third run shows a significant decrease in the catalytic activity.¹⁹ Although no colour change is observed the decrease in catalyst activity indicates decomposition of the air and moisture sensitive manganese complexes, other likely contributions are dilution effects as successive equivalents of Me₂NH·BH₃ substrate are added (solution in 1 mL of toluene), along with build-up of by-products.

It is important to note that whilst no colour change is observed upon the addition of Me₂NH·BH₃ to solutions of precatalysts **1** or **2**, the reaction mixture instantly turns from a colourless solution to a dark suspension when Me₂NH·BH₃ is added to **3**. This observation provides a strong indication of the formation of manganese nanoparticles (NPs), a heterogeneous catalyst for the dehydrocoupling reaction involving precatalyst **3**. The absence of an induction period could indicate that the NPs are formed immediately upon addition of the amine-borane; no induction period was similarly reported by Morris *et al.* in the dehydrogenation of ammonia-borane by iron NPs.²⁰ In order to assess whether the catalysts are homogeneous or heterogeneous the mercury drop test was performed for **1-3** with 5 mol% catalyst loading at 60 °C (entries 1-3, Table 2).²¹ The reactions with precatalysts **1** and **2** in the presence of mercury reached similar conversions to those without after 2 and 4 hours, respectively, indicative of a homogeneous catalyst. Moreover, the presence of an excess of cumene, which can act as a radical trap,^{18, 22} has no effect on the reaction rate and conversion when using precatalysts **1** and **2** indicating that these reactions are not radical mediated. However, when precatalyst **3** is used in the presence of mercury the conversion from Me₂NH·BH₃ to products is considerably lower (Table 2), suggesting that the active catalyst is heterogeneous.^{20, 23} Amine-boranes have been used as effective reducing agents in the chemical synthesis of NPs;²⁴ for instance Me₂NH·BH₃ can be used as a reductant to form Sn, Ni, Pd, Pt and Fe NPs.^{25, 20} This result is, however, unexpected for manganese(II) due to its large negative reduction potential which has made the synthesis of Mn NPs *via* chemical reduction challenging.²⁶

To probe the structure and chemical composition of the heterogeneous catalyst, samples of the reaction mixture were analysed using transmission electron microscopy (TEM), scanning transmission electron microscopy (STEM) and energy dispersive X-ray (EDX) spectroscopy. In an attempt to minimise the potential effect of exposure of the sample to the atmosphere, a few drops of a solution of the catalytically active species, obtained after heating **3** (5 mol%) and Me₂NH·BH₃ in C₆D₆ (0.6 mL) at 60 °C for 16 h and diluting with *ca.* 2 mL benzene, was deposited onto a copper-mounted carbon film under an inert atmosphere. STEM (Figure 5a) and TEM (Figure S2, Supporting Information) images indicate the formation of small ~10 nm Mn NPs, a consequence of the rapid decomposition of the manganese

precatalysts **3** into nanoparticles, which readily assemble into large sub-micron aggregates, consistent with the absence of an effective mechanism for the stabilisation of discrete NPs. Furthermore, EDX spectroscopic analysis (Figure 5b and 5c) confirmed the presence of both manganese (75 at. %) and oxygen (22 at. %), with the apparent excess of manganese indicative of the formation of manganese NPs passivated by a thin layer of a manganese oxide, an artefact of the unavoidable exposure of the sample to atmospheric oxygen during its introduction to the microscope. Complementary analysis of the post-reaction mixture by dynamic light scattering (DLS) indicated that large particles (*ca.* 800-900 nm in hydrodynamic diameter) were indeed present in solution (Figure 5c), supporting the microscopy observations. The apparent offset in determined aggregate size is expected based on fundamental differences in how the absolute value of NP size is determined, with DLS typically overestimating NP size owing to the greater amount of light scattered by larger particles within the distribution.

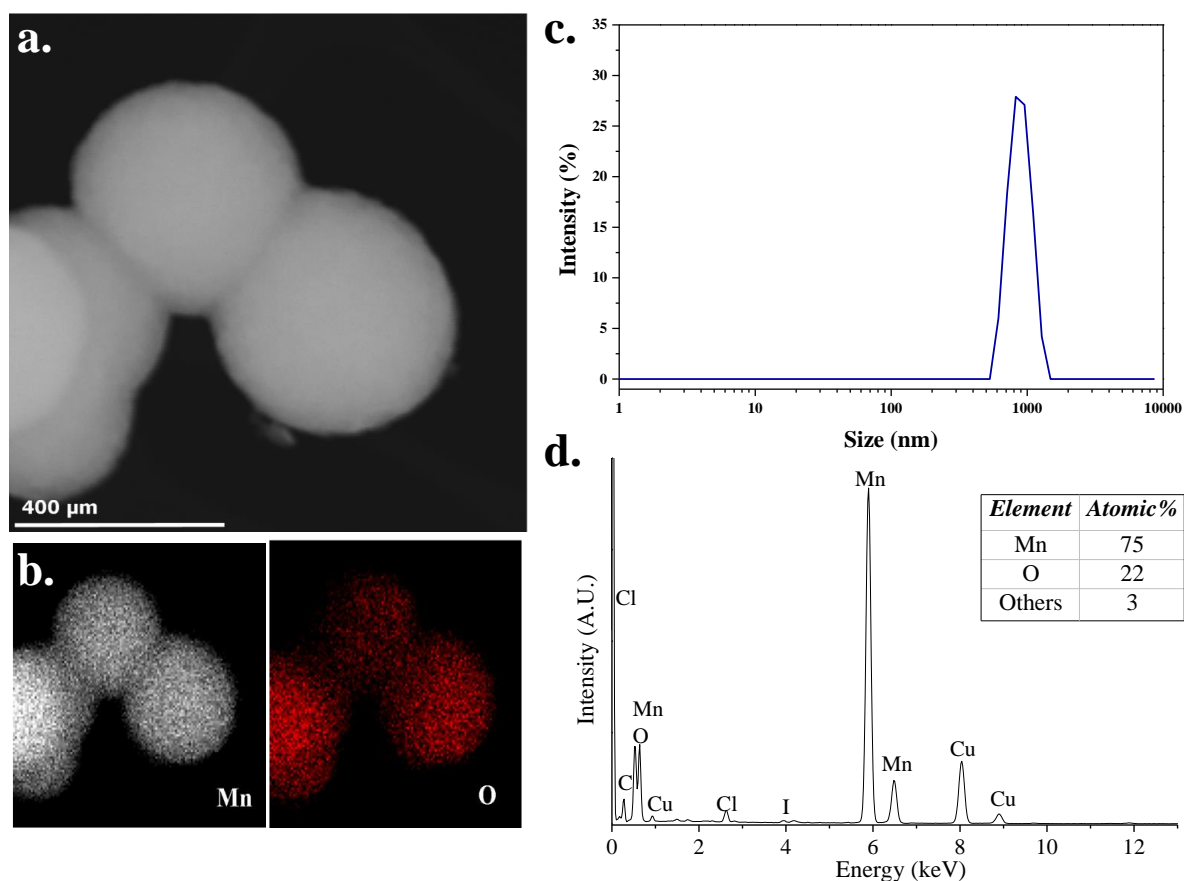


Figure 5. (a) Dark field STEM micrograph of the heterogeneous catalyst. (b) EDX spectroscopic mapping confirming the presence of Mn (white) and O (red) in the NPs. (c) Particle size distribution of hydrodynamic diameter as determined by DLS. (d) Energy dispersive X-ray (EDX) spectrum of manganese NPs on TEM grid with table of atomic % of elements (inset). Copper and carbon peaks originate from the sample support (mesh and film respectively).

Conclusions

Our results indicate that two distinct mechanisms operate when using **1-3** as precatalysts for the dehydrocoupling of $\text{Me}_2\text{NH}\cdot\text{BH}_3$. In the case of **1** and **2** experimental evidence indicates that a homogenous catalyst is the active species, whilst for **3** poisoning experiments together with electron microscopy and light scattering measurements indicate that the true catalyst is heterogeneous and most likely formed from the rapid decomposition of the manganese complex into NPs. However, an important question remains: why do two mechanisms exist (homogeneous vs. heterogeneous) for precatalysts **1-3**? A similar observation has been observed for iron carbonyl complexes in the dehydrocoupling of $\text{Me}_2\text{NH}\cdot\text{BH}_3$ under photoirradiation, where $\text{CpFe}(\text{CO})_2\text{I}$ operates through a homogeneous mechanism and $[\text{CpFe}(\text{CO})_2]_2$ through a heterogeneous mechanism.^{5g} The authors postulate that the low formal oxidation state of Fe(I) could aid the reduction to Fe NPs in the presence of $\text{Me}_2\text{NH}\cdot\text{BH}_3$. However, in **1-3** the manganese centres are in the +II oxidation state, and therefore the difference in reaction mechanisms is more likely due to the steric differences of the ligands. The bulky *m*-terphenyls in **1** and **2** can make the manganese centre resistant to reduction, whilst in contrast, the lower steric demands of the Tmp substituent could render the metal centre in **3** more susceptible to reduction, as reflected in the % V_{Bur} of the *m*-terphenyl ligand.²⁷ In conclusion, two- and three-coordinate manganese *m*-terphenyl complexes are precatalysts for the dehydrocoupling of dimethylamine-borane. Small changes in the ligand used to support the manganese centre produce drastic changes in the reaction mechanism for dehydrocoupling catalysis using *m*-terphenyl precatalysts, indicating that this is an important consideration in the use of these complexes for catalysis.

Experimental

General Methods

All compounds prepared herein are air and moisture sensitive; therefore, all reactions and manipulations were performed by using standard Schlenk line and glovebox equipment under an atmosphere of purified argon or nitrogen. *iso*-hexane (contains <5% *n*-hexane) and *n*-pentane were dried by passing through a column of activated 4 Å molecular sieves. THF and toluene were freshly distilled over sodium benzophenone ketyl (THF) or molten potassium (toluene) under nitrogen. All solvents were degassed *in vacuo* and stored over a potassium mirror (*iso*-hexane, *n*-pentane, toluene) or activated 4 Å molecular sieves (THF) prior to use. Benzene-*d*₆ was dried over potassium and degassed with three freeze/pump/thaw cycles prior to use. NMR spectroscopy were performed on Bruker AV400, AV(III)400, AV(III)400HD or AV(III)600 spectrometers. Chemical shifts are quoted in ppm relative to neat TMS (¹H), and 0.04M $\text{BF}_3\cdot\text{OEt}_2$ (¹¹B). UV/visible spectroscopy was obtained in a Young's tap modified 10 mm quartz cell using a Lambda 750 spectrophotometer. Magnetic moments were calculated using Evans' method.²⁸ $[\text{2,6-Xyl}_2\text{C}_6\text{H}_3\text{Li}]_2$,²⁹ $(\text{2,6-Tmp}_2\text{C}_6\text{H}_3)_2\text{Mn}(\text{THF})^{10}$ and $(\text{2,6-Mes}_2\text{C}_6\text{H}_3)_2\text{Mn}^{11b}$ were prepared following the procedures described in the literature. Elemental microanalysis was performed by Mr. Stephen Boyer at the Microanalysis Service, London Metropolitan University, UK. $\text{Me}_2\text{NH}\cdot\text{BH}_3$ is commercially available and was transferred directly into the glovebox and stored at -30°C. Transmission electron microscopy (TEM) measurements were performed at the Nanoscale and Microscale Research Centre, The University of Nottingham using a JEOL 2100F transmission electron microscope (field emission electron gun source, information limit 0.19 nm). Scanning transmission electron microscopy (STEM) images were acquired using the JEOL digital STEM system. Energy dispersive X-ray (EDX) spectra were recorded using an Oxford Instruments 30mm² Si(Li) detector or an Oxford Instruments x-Max

80 SDD running on an INCA microanalysis system. TEM/STEM/EDX samples were prepared by casting several drops of the reaction mixture onto copper-mesh holey-carbon films and dried under an inert atmosphere. Dynamic light scattering (DLS) measurements were carried out at the Nanoscale and Microscale Research Centre, The University of Nottingham. Samples were prepared as a suspension in dry degassed benzene in a sealed quartz cuvette and intensity particle size distributions acquired using a Malvern Zetasizer Nano-ZS at 25 °C. %V_{Bur} was calculated by employing SambVca and using the metal as the centre of the sphere; default settings were sphere radius 3.5 Å, mesh spacing 0.10 Å, hydrogen atoms included.¹²

Safety warning: Dehydrocoupling of Me₂NH·BH₃ with catalysts **1-3** evolves H₂(g), for the closed systems between 6 and 10 mL of H₂.

Synthesis of (2,6-Xyl₂C₆H₃)₂Mn (**1**)

Toluene (30 mL) and THF (3 mL) were added to a mixture of [2,6-Xyl₂C₆H₃Li]₂ (500 mg, 0.860 mmol) and MnBr₂ (183 mg 0.860 mmol) and stirred overnight at room temperature. The solvent was removed *in vacuo* and the resulting pale off white solid was extracted into toluene (20 mL). Filtration and storage at -30 °C for 24 hours resulted in pale pink crystals suitable for X-ray diffraction studies (144 mg, 27%). ¹H NMR (C₆D₆, 400 MHz, 25 °C): δ_H / ppm -6.26 (s, br, Δv_{1/2} = 1020 Hz) 0.40 (s) 0.97 (s) 10.34 (s, br, Δv_{1/2} = 1200 Hz) 15.55 (s, br, Δv_{1/2} = 5600 Hz) 26.35 (s, br, Δv_{1/2} = 2832 Hz). μ_{eff} (Evans, C₆D₆, 25 °C = 5.32 μB. UV/Vis (THF) λ_{max}/nm (ε/dm³ mol⁻¹ cm⁻¹): 369 (141), 356 (207), 322 (429). MS (ESI) *m/z*: calcd for C₄₄H₄₂Mn [M+H]⁺ 626.2742, found: 626.2745 (err [ppm] = 0.50). Elemental analysis C₄₄H₄₂Mn (625.758): calcd. C 84.46 H 6.77; found C 84.31, H 6.54 %.

Standard procedure for the catalytic dehydrocoupling of Me₂NH·BH₃

In a Young's NMR tube 5 or 2 mol% of precatalyst (**1-3**) and Me₂NH·BH₃ were dissolved in C₆D₆ (0.6 mL). The reactions were either carried out at room temperature or heated to 60 °C in a sealed NMR tube (closed system). Conversion was quantified by integration of ¹H and ¹¹B NMR spectra. See Table S1 (supporting information) for quantities of reagents used.

Standard procedure for the catalytic dehydrocoupling of Me₂NH·BH₃ monitored by H₂ evolution

7 mol% of precatalyst **2** (57.0 mg, 0.0835 mmol) was dissolved in toluene (3.5 mL) under argon in a Schlenk flask connected to a gas burette filled with paraffin oil. The reaction was heated to 60 °C and, after the vapour pressure of the solvent was reached, 1 mL of a toluene solution of Me₂NH·BH₃ (70.1 mg, 1.19 mmol) was syringed into the reaction vessel *via* a silicon septum. The mixture was stirred (400 rpm) during the run. Upon injection, the reaction was monitored measuring the volume increase in the gas burette, zeroing the data to the point where the volume of oil began to decrease. To test the recyclability of the system, a second and third loading of Me₂NH·BH₃ (70.1 mg, 1.19 mmol) dissolved in toluene (1 mL) were syringed into the reaction *via* a silicon septum when the catalysis was finished and monitored by H₂ evolution. It must be noted that upon addition of successive Me₂NH·BH₃ loadings the volume increases, from 3.5 mL (first run) to 4.5 mL (second run) and 5.5 mL (third run), leading to a decrease in the concentration of the catalyst and therefore can account for some of the decrease in catalyst activity.

Standard procedure for *in situ* NMR reaction monitoring for the catalytic dehydrocoupling of Me₂NH·BH₃

In a Young's NMR tube 5 mol% of precatalyst (**1-3**) was dissolved in C₆D₆ (0.6 mL) and cooled to -30 °C after which Me₂NH·BH₃ in C₆D₆ (0.2 mL) was added and the sample cooled to -78 °C to prevent the reaction from initiating. The sample was transferred to the NMR spectrometer and monitored directly at 60 °C. Conversion was quantified by integration of ¹H and ¹¹B NMR spectra. See Table S1 for quantities of reagents used.

Mercury drop test

In a Young's NMR tube 5 mol% of precatalyst (**1-3**) and Me₂NH·BH₃ were dissolved in C₆D₆ (0.6 mL), hydrogen bubbles were immediately observed. After 5 min., Hg (*ca.* 1 drop) was added to the reaction and it was heated at 60 °C. The reaction was monitored by ¹H and ¹¹B NMR at the times indicated in Table 2. See Table S1 for quantities of reagents used.

Radical Trap Test

In a Young's NMR tube 5 mol% of precatalyst **1** or **2** was dissolved in C₆D₆ (0.4 mL) with cumene (**1**: 11 μL, 0.0800 mmol; **2**: 10 μL, 0.0735 mmol) and cooled to -30 °C after which Me₂NH·BH₃ in C₆D₆ (0.2 mL) was added and the sample cooled to -78 °C to prevent the reaction from initiating. The sample was transferred to the NMR spectrometer and monitored directly at 60 °C. Conversion was quantified by integration of ¹H and ¹¹B NMR spectra. See Table S1 for quantities of reagents used.

Transmission electron microscopy (TEM)

The sample for TEM analysis was prepared under a nitrogen atmosphere in a glove box. The reaction solution of **3** (5 mol% catalyst loading) and Me₂NH·BH₃ in C₆D₆ (0.6 mL), after heating at 60 °C for 16 h, was diluted with *ca.* 2 mL of benzene. An aliquot of this solution was spotted onto a lacey carbon coated copper grid and the solvent allowed to evaporate. The grid was then transferred to the TEM holder under an inert atmosphere after which the air tight cover was placed on the holder. The TEM holder was quickly put inside the TEM microscope, resulting in the exposure of the sample in air for *ca.* 5 seconds until high vacuum was achieved.

Conflicts of interest

There are no conflicts to declare.

Acknowledgements

We gratefully acknowledge the support of the University of Nottingham, the EPSRC and Leverhulme Trust. We also thank Dr. Huw Williams and Mr. Rhys Lodge, University of Nottingham for helpful discussions and Mr. Stephen Boyer (London Metropolitan University) for elemental analyses.

Notes and references

1. a) S. Bhunya, T. Malakar, G. Ganguly and A. Paul, *ACS Catal.*, 2016, **6**, 7907; b) E. M. Leitao, T. Jurca and I. Manners, *Nat. Chem.*, 2013, **5**, 817; c) A. Staubitz, A. P. M. Robertson and I. Manners, *Chem. Rev.*, 2010, **110**, 4079; d) A. Staubitz, A. P. M. Robertson, M. E. Sloan and I. Manners, *Chem. Rev.*, 2010, **110**, 4023.
2. a) E. M. Leitao, N. E. Stubbs, A. P. Robertson, H. Helten, R. J. Cox, G. C. Lloyd-Jones and I. Manners, *J. Am. Chem. Soc.*, 2012, **134**, 16805; b) Y. Jiang, O. Blacque, T. Fox, C. M. Frech and H. Berke, *Organometallics*, 2009, **28**, 5493.
3. a) J. C. Koepke, J. D. Wood, Y. Chen, S. W. Schmucker, X. Liu, N. N. Chang, L. Nienhaus, J. W. Do, E. A. Carrion, J. Hewaparakrama, A. Rangarajan, I. Datye, R. Mehta, R. T. Haasch, M. Gruebele, G. S. Girolami, E. Pop and J. W. Lyding, *Chem. Mater.*, 2016, **28**, 4169; b) H. C. Johnson, E. M. Leitao, G. R. Whittell, I. Manners, G. C. Lloyd-Jones and A. S. Weller, *J. Am. Chem. Soc.*, 2014, **136**, 9078; c) S. Frueh, R. Kellett, C. Mallery, T. Molter, W. S. Willis, C. King'ondeu and S. L. Suib, *Inorg. Chem.*, 2011, **50**, 783.
4. a) M. A. Esteruelas, P. Nolis, M. Olivan, E. Oñate, A. Vallribera and A. Velez, *Inorg. Chem.*, 2016, **55**, 7176; b) A. Kumar, N. A. Beattie, S. D. Pike, S. A. Macgregor and A. S. Weller, *Angew. Chem. Int. Ed.*, 2016, **55**, 6651; c) M. A. Esteruelas, A. M. López, M. Mora and E. Oñate, *ACS Catal.*, 2015, **5**, 187; d) M. Rosello-Merino, J. Lopez-Serrano and S. Conejero, *J. Am. Chem. Soc.*, 2013, **135**, 10910; e) L. J. Sewell, G. C. Lloyd-Jones and A. S. Weller, *J. Am. Chem. Soc.*, 2012, **134**, 3598.
5. a) F. Anke, D. Han, M. Klahn, A. Spannenberg and T. Beweries, *Dalton Trans.*, 2017, **46**, 6843; b) N. T. Coles, M. F. Mahon and R. L. Webster, *Organometallics*, 2017, **36**, 2262; c) A. Glüer, M. Förster, V. R. Celinski, J. Schmedt auf der Günne, M. C. Holthausen and S. Schneider, *ACS Catal.*, 2015, **5**, 7214; d) C. Lichtenberg, L. Viciu, M. Adelhardt, J. Sutter, K. Meyer, B. de Bruin and H. Grützmacher, *Angew. Chem. Int. Ed.*, 2015, **54**, 5766; e) A. Schafer, T. Jurca, J. Turner, J. R. Vance, K. Lee, V. A. Du, M. F. Haddow, G. R. Whittell and I. Manners, *Angew. Chem. Int. Ed.*, 2015, **54**, 4836; f) P. Bhattacharya, J. A. Krause and H. Guan, *J. Am. Chem. Soc.*, 2014, **136**, 11153; g) J. R. Vance, A. Schafer, A. P. Robertson, K. Lee, J. Turner, G. R. Whittell and I. Manners, *J. Am. Chem. Soc.*, 2014, **136**, 3048; h) R. T. Baker, J. C. Gordon, C. W. Hamilton, N. J. Henson, P. H. Lin, S. Maguire, M. Murugesu, B. L. Scott and N. C. Smythe, *J. Am. Chem. Soc.*, 2012, **134**, 5598.
6. a) S. Todisco, L. Luconi, G. Giambastiani, A. Rossin, M. Peruzzini, I. E. Golub, O. A. Filippov, N. V. Belkova and E. S. Shubina, *Inorg. Chem.*, 2017, **56**, 4296; b) J. K. Pagano, J. P. Stelmach and R. Waterman, *Dalton Trans.*, 2015, **44**, 12074; c) T. P. Lin and J. C. Peters, *J. Am. Chem. Soc.*, 2013, **135**, 15310.
7. a) S. Muhammad, S. Moncho, E. N. Brothers and A. A. Bengali, *Chem. Commun.*, 2014, **50**, 5874; b) T. Kakizawa, Y. Kawano, K. Naganeyama and M. Shimoi, *Chem. Lett.*, 2011, **40**, 171.
8. M. Gediga, C. M. Feil, S. H. Schlindwein, J. Bender, M. Nieger and D. Gudat, *Chem. Eur. J.*, 2017, **23**, 11560
9. a) W. Liu and L. Ackermann, *ACS Catal.*, 2016, **6**, 3743; b) D. A. Valyaev, G. Lavigne and N. Lugan, *Coord. Chem. Rev.*, 2016, **308**, 191; c) J. Emsley, *Nature's Building Blocks: An A–Z. Guide to the Elements - Manganese*, Oxford University Press, Oxford, 2001.
10. H. R. Sharpe, A. M. Geer, H. E. Williams, T. J. Blundell, W. Lewis, A. J. Blake and D. L. Kays, *Chem. Commun.*, 2017, **53**, 937.
11. a) C. Ni, J. C. Fettingler, G. J. Long and P. P. Power, *Dalton Trans.*, 2010, **39**, 10664; b) D. L. Kays and A. R. Cowley, *Chem. Commun.*, 2007, **10**, 1053.

12. L. Falivene, R. Credendino, A. Poater, A. Petta, L. Serra, R. Oliva, V. Scarano and L. Cavallo, *Organometallics*, 2016, **35**, 2286.
13. M. E. Sloan, A. Staubitz, T. J. Clark, C. A. Russell, G. C. Lloyd-Jones and I. Manners, *J. Am. Chem. Soc.*, 2010, **132**, 3831.
14. M. S. Hill, G. Kociok-Kohn and T. P. Robinson, *Chem. Commun.*, 2010, **46**, 7587.
15. H. C. Johnson, A. P. Robertson, A. B. Chaplin, L. J. Sewell, A. L. Thompson, M. F. Haddow, I. Manners and A. S. Weller, *J. Am. Chem. Soc.*, 2011, **133**, 11076.
16. a) C. A. Jaska, K. Temple, A. J. Lough and I. Manners, *J. Am. Chem. Soc.*, 2003, **125**, 9424; b) C. A. Jaska, K. Temple, A. J. Lough and I. Manners, *Chem. Commun.*, 2001, 962.
17. C. Ni, H. Lei and P. P. Power, *Organometallics*, 2010, **29**, 1988.
18. H. R. Sharpe, A. M. Geer, W. Lewis, Alexander J. Blake and D. L. Kays, *Angew. Chem. Int. Ed.*, 2017, **56**, 4845.
19. Rate constants could not be determined due to solubility problems at catalyst loadings higher than 7 mol%.
20. J. F. Sonnenberg and R. H. Morris, *ACS Catal.*, 2013, **3**, 1092.
21. a) R. H. Crabtree, *Chem. Rev.*, 2012, **112**, 1536; b) J. A. Widegren and R. G. Finke, *J. Mol. Catal. A: Chem.*, 2003, **198**, 317.
22. K. J. Gallagher and R. L. Webster, *Chem. Commun.*, 2014, **50**, 12109.
23. M. Zahmakiran and S. Ozkar, *Inorg. Chem.*, 2009, **48**, 8955.
24. S. B. Kalidindi, U. Sanyal and B. R. Jagirdar, *ChemSusChem*, 2011, **4**, 317.
25. O. Lidor-Shalev and D. Zitoun, *RSC Adv.*, 2014, **4**, 63603.
26. J. F. Bondi, K. D. Oyler, X. Ke, P. Schiffer and R. E. Schaak, *J. Am. Chem. Soc.*, 2009, **131**, 9144.
27. R. C. Smith, T. Ren and J. D. Protasiewicz, *Eur. J. Inorg. Chem.*, 2002, 2779.
28. D. F. Evans, *J. Chem. Soc.*, 1959, 2003.
29. S. Hino, M. M. Olmstead, J. C. Fettinger and P. P. Power, *J. Organomet. Chem.*, 2005, **690**, 1638.